Science Academique

Science Academique
Rifana BA, et al.
Pages: 44-49

Research Article

Quantum Computational, Spectroscopy Investigation (FTIR, FT-Raman), HOMO-LUMO and Docking Studies on Selegiline

B. Aysha Rifana[1,2], Shyam Sundar[1], Johanan Christian Prasana[1,2*], A. Anuradha[2,3]

[1]Department of Physics, Madras Christian College, East Tambaram, Chennai, 600059, Tamil Nadu, India
[2]University of Madras, Chennai, 600005, Tamil Nadu, India
[3]PG & Research Department of Physics, Queen Mary's College, Chennai, 600004, Tamil Nadu, India

[*]**Correspondence to:** Johanan Christian Prasana; reachjcp@gmail.com

Citation: Rifana BA, Sundar S, Prasana JC, Anuradha A (2022) Quantum Computational, Spectroscopy Investigation (FTIR, FT-Raman), HOMO-LUMO and Docking Studies on Selegiline. Sci Academique 3(2): 44-49

Received: 20 September, 2022; **Accepted:** 04 October 2022; **Publication:** 08 October 2022

Abstract
Computational analysis has been a powerful tool in characterizing a compound. With its high precision, accurate results can be obtained for any given compound. Density Functional Theory, a quantum mechanical computational method was used to study vibrational spectra of the title compound. Relative and absolute values of FTIR and FT-Raman were found. Potential energy distribution percentage for each vibrational mode was calculated. The calculated HOMO and LUMO energies were -6.1022 eV and -0.4493 eV, respectively, resulting in a band gap energy of 5.6529 eV, indicating charge transfer within the molecule. UV spectra of the title compound were observed by TD-DFT method. Electron localization function (ELF), Localized orbital locator (LOL), Molecular electrostatic potential (MEP) of the title compound were also obtained. Drug likeness values were analyzed to assess the title compound's potential as an active pharmaceutical component. Biological nature of the compound was observed by molecular docking studies.

Introduction

Monoamine oxidase (MAO), discovered by Balschko in the 1930s, is one of the most important enzymes in neurotransmitter metabolism [1]. MAO has the potential to be used in the treatment of several neurodegenerative diseases, including Parkinson's and Alzheimer's. MAO-catalyzed reactions generate hydrogen peroxide, a source of hydroxyl radicals, and MAO inhibitors may thus be useful in managing the outcome of stroke and other tissue damage caused by oxidative stress [2]. Selegiline (title compound) was developed in Hungary by Knoll et al. in 1964 as a novel monoamine oxidase (MAO)-inhibitor antidepressant. In patients with early Parkinson's disease (PD), Selegiline postpones the need for levodopa therapy [3]. From the deprenyl and tocopherol antioxidative treatment, selegiline, with or without tocopherol, reduces physical and psychological

deficits in patients with PD within first month of treatment and reduces the probability of reaching a primary endpoint, the decision to treat with levodopa [4]. The empirical formula of selegiline is C13H17N, and IUPAC name is ethyl (2R)-N-methyl-1-Phenyl-N-prop-2-ynylpropan-2-amine.

According to literature survey, a few spectroscopic and in vitro assays have already been published on the title compound [5,6]. The present study provides a complete vibrational, electronic and topological analysis under theoretical background. This paper describes a comprehensive spectroscopic investigation of the title compound at the B3LYP/6-311++G (d, p) level of theory. Frontier molecular orbitals (HOMO, LUMO) determine how the molecule interacts with other species, allowing us to characterize the chemical reactivity of the molecule. MEP (Molecular Electrostatic potential), ELF (Electron localization function) and LOL (Localized orbital locator) were used to examine the distribution of electrons and reactive sites on the surface of the title compound. Drug likeness were also carried out. Molecular docking analysis is performed by selecting suitable protein targets to study the bio activeness of the title compound.

Computational Details

The molecular parameters of the title compound in ground state were calculated using DFT B3LYP/6-311++G (d, p) basis set. In DFT methods, Becke's three(B3) combined with Lee, Yang and Parr(LYP) method is the best predicting results for molecular geometry and vibrational wave numbers for moderately larger molecule [7,8]. Chemcraft 1.8 [9] was used to visualize optimized geometrical structure of the title compound. Vibrational assignment calculations in terms of PED contributions were performed with high accuracy using VEDA software. [10]. Molecular electrostatic potential (MEP) and HOMO-LUMO studies were carried out using Gauss View 5.0software [11-13]. Localized Orbital Locator (LOL) and Electron Localization Function (ELF) two-dimensional plots were obtained using MULTIWFN 3.4.1 [14]. Swiss ADME Tool is used to determine the drug likeness nature and ADME properties of the title compound [15]. The binding energy, inhibition constant, and other biological parameters of ligand-protein interaction were determined using the AutoDock 4.2.1 programme [16].

Results and Discussion

Molecular Geometry

Bond parameters (bond angle and bond length) of the title compound were obtained by DFT/B3LYP method with basis set 6-311++G (d, p). The optimized geometrical structure is shown in Fig. 1. Bond angle, the angle between three atoms and bond length, the distance between two neighboring atoms values obtained were tabulated in table 1. Homonuclear atoms such as C12-C15, C15-C17 and C6-C12 have the highest bond lengths of 1.553 Å, 1.532 Å and 1.513 Å. On the other hand, heteronuclear atoms such as C15-N21, N21-C26 and N21-C22 have the highest bond lengths of 1.483 Å,1.470 Å and 1.463 Å. Least bond length values were found in atoms C30-H3, C3-H9 and C1-H7 of values 1.063,1.084 and 1.085. In the case of bond angle, the maximum values obtained were 121.3°, 121.1° and 121.1° which corresponded to the atoms C1-C6-C12, C4-C5-C6 and C2-C1-C6 respectively. Presence of benzene ring structure comprised of atoms C1 to C6 was observed in the title compound.

Science Academique
Rifana BA, et al.
Pages: 44-49

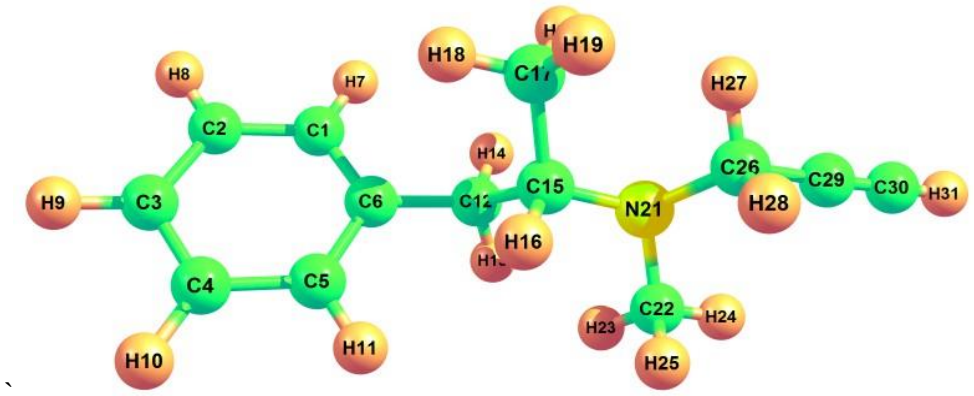

Figure 1: Optimised geometric structure of (2R)-N-methyl-1-Phenyl-N-prop-2-ynylpropan-2-amine.

Bond Length (Å)	B3LYP/6-311++G (d, p)	Bond Angle (°)	B3LYP/6-311++G (d, p)
C1-C2	1.399	C2-C1-C6	121.1
C1-C6	1.399	C2-C1-H7	119.6
C1-H7	1.085	C1-C2-C3	120.1
C2-C3	1.393	C1-C2-H8	119.8
C2-H8	1.085	C6-C1-H7	119.3
C3-C4	1.395	C1-C6-C5	118.1
C3-H9	1.084	C1-C6-C12	121.3
C4-C5	1.393	C3-C2-H8	120.1
C4-H10	1.085	C2-C3-C4	119.4
C5-C6	1.401	C2-C3-H9	120.3
C5-H11	1.086	C4-C3-H9	120.3
C6-C12	1.513	C3-C4-C5	120.2
C12-H13	1.091	C3-C4-H10	120.0
C12-H14	1.094	C5-C4-H10	119.8
C12-C15	1.553	C4-C5-C6	121.1
C15-H16	1.106	C4-C5-H11	119.4
C15-C17	1.532	C6-C5-H11	119.5
C15-N21	1.483	C5-C6-C12	120.6
C17-H18	1.091	C6-C12-H13	108.4
C17-H19	1.091	C6-C12-H14	110.2
C17-H20	1.095	C6-C12-H15	114.3
N21-C22	1.463	C3-C12-14	106.4
N21-C26	1.470	H13-C12-C15	109.6
C22-H23	1.089	H14-C12-C15	107.8
C22-H24	1.090	C12-C15-H16	108.1
C22-H25	1.106	C12-C15-C17	109.2
C26-H27	1.089	C12-C15-N21	109.1
C26-H28	1.108	H16-C15-C17	107.6
C26-C29	1.464	H16-C15-N21	109.3
C29-C30	1.202	C17-C15-N21	113.4
C30-H31	1.063	C15-C17-H18	109.2

		C15-C17-H19	112.8
		C15-C17-H20	110.9
		C15-N21-C22	111.8
		C15-N21-C26	114.1
		H18-C17-H19	107.0
		H18-C17-H20	108.0
		H19-C17-H20	108.8
		C22-N21-C26	109.8
		N21-C22-H23	111.0
		N21-C22-H24	109.6
		N21-C22-H25	112.2
		N21-C26-H27	109.2
		N21-C26-H28	112.0
		N21-C26-C29	113.0
		H23-C22-H24	107.5
		H23-C22-H25	108.2
		H24-C22-H25	108.3
		H27-C26-H28	106.8
		H27-C26-C29	107.3
		H28-C26-C29	108.3
		C26-C29-C30	178.0
		C29-C30-H31	179.6

Table 1: Geometrical parameters Bond Length (Å) and Bond Angle (°) optimized in (2R)-N-methyl-1-Phenyl-N-prop-2-ynylpropan-2-amine with basis set 6-311++G (d, p).

Vibrational Analysis

Vibrational analysis of the title compound was carried out in detail through FT-IR and FT-RAMAN studies. For a non-linear compound, the title compound will have n = 3N-6 normal vibrational modes, i.e., n = 87. The contribution of vibrational frequency by a particular set towards the potential energy were represented as potential energy distribution (PED%) and their values are tabulated in table 2 [17]. A factor of 0.961 was multiplies to the unscaled frequency values to get the scaled values as they are more refined and accurate. Types of vibration such as stretching, bending and torsional were given by the vibrational assignment. All vibrational calculations were carried out by GAUSSIAN 09W with basis set, B3LYP/6-311++G (d, p). fig.2 and fig.3 represents the theoretical FT-IR and FT-RAMAN spectra.

C-H Vibration

Heteroaromatic organic compound and its derivatives commonly exhibit multiple peaks in the region 3100 to 3000 cm^{-1} [18,19]. The C-H stretching bands of the title compound was reported in the range 3340 to 2773 cm^{-1}. The highest Stretching 98% was observed in the vibrational region of 2911 cm^{-1} and 2693 cm^{-1}. Pure stretching was not found in any region.

C-C Vibration

The bonds between 1650 and 140 cm^{-1} range in the aromatic and heteroaromatic compounds are assigned to carbon-carbon vibration [20]. In the present study, Theoretical frequencies assigned to C-C stretching vibrations are 2131 cm^{-1},1591 cm^{-1} and maximum PED contribution to this vibration is 96%.

C-N Vibration

Mixing of several modes is possible in the region makes the documentation of C-N bonds very difficult. Frequency nearer to 1500 cm^{-1}

indicates C=N bonds while frequency nearer to 1300 cm^{-1} indicates the presence of C-N bonds [21]. For the title compound, C-N stretching vibrations were found at 1201 ,1127 ,1041 ,974, 914 and 777 cm^{-1}.

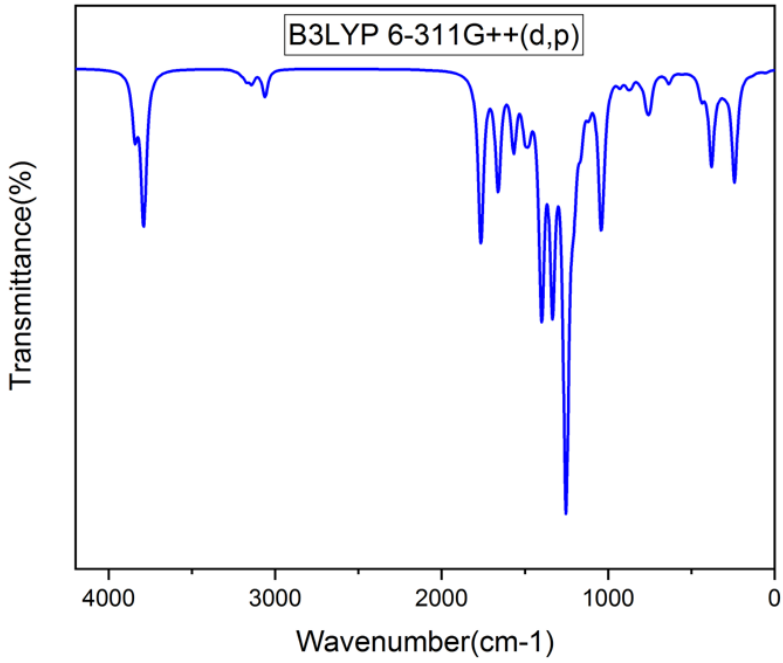

Figure 2: FT-IR Spectra**.**

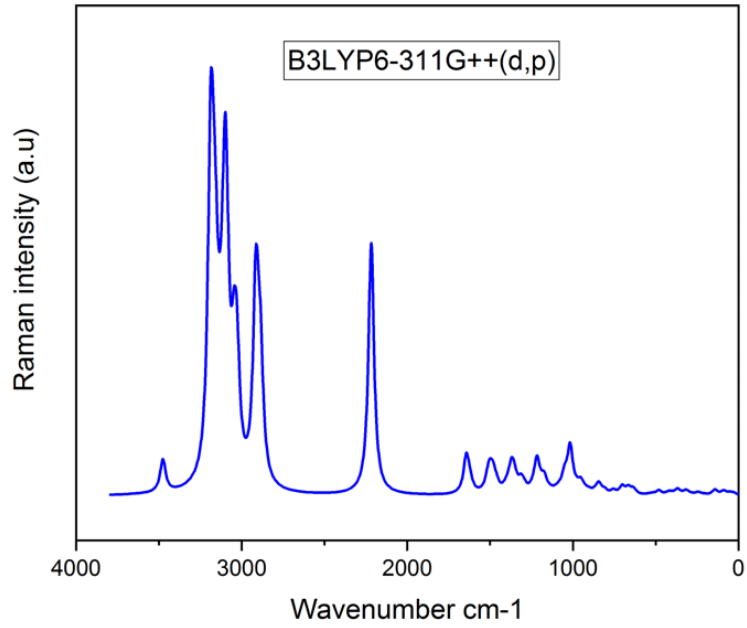

Figure 3: FT-RAMAN Spectra.

Science Academique
Rifana BA, et al.
Pages: 44-49

Modes	CM-1		IR Intensity		Raman Activity		Vibrational Assignment PED%
	Unscaled	Scaled	Relative	Absolute	Relative	Absolute	
87	3476	3340	77	62	37	10	STRE CH(95)
86	3187	3063	16	13	325	100	STRE CH(94)
85	3176	3052	31	25	44	12	STRE CH(93)
84	3167	3044	7	6	111	31	STRE CH(93)
83	3156	3033	3	3	66	19	STRE CH(86)
82	3152	3029	9	7	32	9	STRE CH(90)
81	3129	3007	25	20	38	1	STRE CH(94)
80	3112	2991	24	20	31	9	STRE CH(95)
79	3104	2983	7	6	128	36	STRE CH(89)
78	3097	2976	18	15	63	18	STRE CH(91)
77	3094	2974	33	26	145	41	STRE CH(87)
76	3083	2963	8	6	24	7	STRE CH(98)
75	3047	2928	18	15	94	27	STRE CH(97)
74	3029	2911	19	15	114	32	STRE CH(98)
73	2915	2801	123	100	194	55	STRE CH(96)
72	2902	2789	31	25	50	14	STRE CH(97)
71	2886	2773	53	43	108	31	STRE CH(96)
70	2218	2131	4	3	282	80	STRE CC(96)
69	1643	1579	9	7	42	12	STRE CC(38)
68	1621	1558	1	1	10	3	STRE CC(50)+BEND CCC(12)
67	1526	1466	12	10	1	0	BEND HCC(69)+BEND CCC(10)
66	1518	1459	8	7	4	1	BEND HCH(68)+TORS HCCC(13)
65	1508	1449	14	11	12	4	BEND HCH(69)+TORS HCNC(10)
64	1502	1444	6	5	4	1	BEND HCH(66)
63	1501	1443	5	4	8	2	BEND HCH(39)
62	1487	1429	3	2	9	3	BEND HCH(55)
61	1480	1423	4	3	4	1	BEND HCH(33)
60	1480	1422	2	2	8	2	BEND HCC(10)+BEND HCH(56)
59	1461	1404	4	3	7	2	BEND HCH(89)
58	1412	1357	19	15	2	0	BEND HCH(83)
57	1395	1341	9	8	6	2	BEND HCC(24)
56	1377	1323	11	9	5	2	BEND HCC(43)
55	1368	1315	25	20	24	7	TORS HCCC(17)+TORS HCNC(23)
54	1353	1300	8	7	12	3	BEND HCC(35)+TORS HCNC(21)
53	1337	1285	2	1	1	0	STRE CC(69)

52	1312	1261	1	1	12	3	BEND HCC(24)+TORS HCCC(36)+TORS HCNC(11)
51	1294	1244	8	7	5	1	BEND HCC(31)+TORS HCNC(22)
50	1250	1201	42	34	1	0	STRE NC(13)+BEND HCC(10)+TORS HCNC(15)
49	1238	1190	5	4	3	1	BEND HCC(12)+TORS HCCC(12)+TORS HCCC(11)
48	1218	1170	11	9	35	10	STRE CC(28)+TORS HCCC(12)
47	1203	1156	0	0	4	1	STRE CC(10)+BEND HCC(73)
46	1181	1135	0	0	3	1	BEND HCC(75)
45	1173	1127	16	13	13	4	STRE NC(22)+BEND HCC(19)
44	1144	1099	14	11	2	1	BEND HCH(16)+TORS HCNC(56)
43	1123	1079	24	19	1	0	BEND HCC(10)+TORS HCCC(10)
42	1100	1057	12	10	2	1	TORS HCCC(11)
41	1083	1041	28	23	3	1	STRE NC(51)+STRECC(10)
40	1060	1019	2	1	1	0	BEND HCC(15)+ TORS HCCC(18)
39	1050	1009	5	4	17	5	STRE CC(41)
38	1017	977	0	0	46	13	STRE CC(22)+BEND CCC(61)
37	1013	974	26	21	5	2	STRE CC(13)+STRE NC(15)+TORS HCCC(12)+TORS CCCN(14)
36	1000	961	0	0	0	0	TORS HCCC(66)+TORS CCCC(14)
35	984	945	0	0	0	0	TORS HCCC(89)
34	976	938	18	14	4	1	STRE CC(12)+TORS HCCC(46)+TORS CCCN(18)
33	951	914	7	6	11	3	STRE CC(34)+STRE NC(13)
32	928	892	2	1	3	1	TORS HCCC(68)
31	902	867	5	4	3	1	STRE CC(17)+ TORSHCCC(15)
30	867	833	5	4	2	1	STRE CC(29)+TORS HCCC(14)
29	856	823	0	0	0	0	TORS HCCC(98)
28	843	810	3	2	11	3	STRE CC(10)+BEND CCC(15)
27	808	777	11	9	4	1	STRE NC(29)+BEND CCC(14)
26	755	725	31	25	4	1	TORS HCCC(44)+TORS CCCC(15)
25	714	686	41	33	0	0	TORS HCCC(26)+ TORS CCCC(36)+OUT CCCC(12)
24	701	674	44	35	9	2	BEND HCC(87)+TORS HCCC(10)

23	664	638	53	43	7	2	BEND HCCC(10)+TORS HCCC(88)
22	636	612	0	0	4	1	BEND CCC(16)+BEND CCC(54)
21	628	604	5	4	2	1	BEND CCN(11)
20	543	522	2	1	1	0	BEND CCC(12)+BEND CCN(15)
19	518	498	11	9	1	0	OUT CCCC(24)
18	480	461	1	1	5	1	STRE CC(12)+BEND CNC(21)+BEND CCN(16)
17	428	411	2	1	2	0	BEND CCN(25)
16	415	399	0	0	0	0	TORS HCCC(12)+TORS CCCC(68)
15	411	395	3	2	2	1	BEND CCC(15)+BEND CNC(48)
14	372	357	7	6	4	1	TORS CCCN(18)+OUT CCCN(20)
13	362	348	1	1	3	1	BEND CCC(20)+TORS HCCC(21)
12	321	308	2	2	3	1	TORS HCCC(40)+TORS CCCN(15)
11	309	297	2	1	3	1	BEND CCC(20)+BEND CNC(11)+ TORS HCCC(10)+OUT CCCN(16)+OUT CCNC(10)
10	281	270	0	0	1	0	BEND CNC(12)+BEND CCN(22)+TORS HCCC(20)
9	247	238	0	0	2	0	STRE CC(12)+BEND CCC(10)+BEND NCC(28)
8	237	228	2	1	2	0	BEND CCC(14)+TORS CCCC(32)
7	205	197	1	1	1	0	TORS HCNC(70)
6	142	136	1	0	6	2	BEND CCC(35)+BEND CCN(29)
5	92	89	0	0	2	1	BEND CCC(28)+OUT CCCC(20)
4	84	81	0	0	2	1	TORS CCNC(61)
3	50	48	0	0	2	1	TORS NCCC(12)+TORS CCCC(44)+OUT CCCC(12)
2	30	29	0	0	0	0	TORS CCNC(23)+TORS CNCC(20)+TORS NCCC(22)+OUT CCCN(12)
1	26	25	0	0	2	1	TORS CNCC(14)+TORS NCCC(50)+TORS CCCC(15)

Table 2: Theoretical vibrational spectroscopic data with vibrational assignments for title compound using DFT B3LYP/6-311++G (d, p) basis set.

Science Academique
Rifana BA, et al.
Pages: 44-49

Frontier Molecular Orbital

Frontier molecular analysis was carried out for the title compound using DFT method along with B3LYP/6-311++G (d, p) to understand the interactions of the molecule with other molecules. Highest Occupied Molecular Orbital (HOMO) and Lowest Unoccupied Molecular Orbital (LUMO) is derived from FMO analysis. Transition between HOMO whose energy is less as they are at ground state to LUMO whose energy levels are high as they constitute excited states gives us the values of Energy Band Gap (eV) shown in fig. 4 [22,23]. Whilst Homo are electron donors, the LUMO is more electronegative in nature. High electron affinities values denote that the molecular interactions are strong. Electronegativity deals with the tendency of the molecule to accept more electrons. The energy gap between two states plays a vital role as many other parameters such as electron affinity, ionization potential, chemical softness and are tabulated in table 4. Chemical softness and chemical hardness were found to be 0.17689 η and 2.8265 S. HOMO and LUMO values characterizes the chemical kinetics stability of the title compound. For shorter energy gaps, the compound is polarized, and they are called as soft molecules [24].

Basis Set	B3LYP/6-311++G (d, p)
E_{LUMO}(eV)	-0.4493
E_{HUMO}(eV)	-6.1022
Ionization potential(I)	6.1022
Electron affinity(A)	0.4493
Energy gap(eV)	5.6529
Electronegativity(χ)	3.2757
Chemical potential(μ)	-3.2757`
Chemical hardness(η)	2.8265
Chemical softness(S)	0.1769

Table 4: Calculated energies values of the title compound

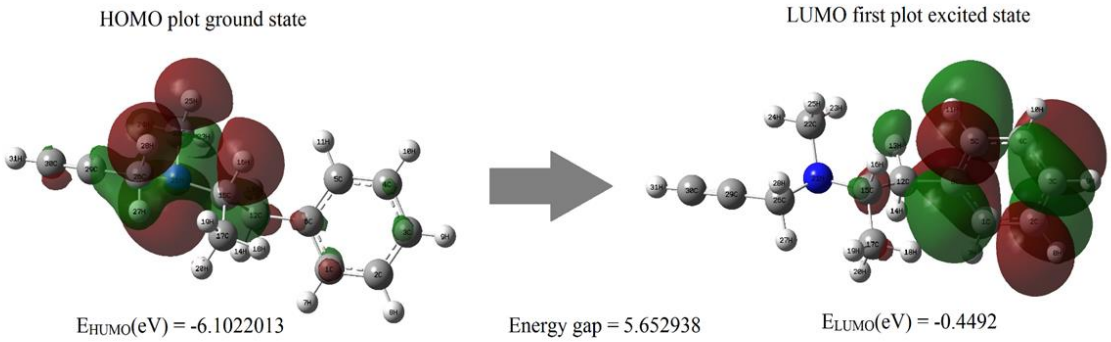

Figure 4: The molecular orbitals and energies for HOMO and LUMO of ethyl (2R)-N-methyl-1-phenyl-N-prop-2-ynylpropan-2-amine.

UV – Visible Spectral Analysis

UV spectrum of the title compound was obtained from GAUSSUM software. Time dependent DFT was carried out to visualise the effect of solvent to aqueous phase of the title compound. The study was carried out in solvent phase in solvent model density (SDM). Through the computational method, the values of maximum wavelength λ_{max} (nm), Band gap energy(eV), excitation energy (cm^{-1}), and oscillator strength (f) of the title compound were obtained and tabulated in table 5 [25]. The band gap was calculated using the formula E = hc/λ. UV spectral analysis show the electronic absorption which excites the atom from highest occupied molecular orbital (HOMO) to lowest unoccupied molecular orbital (LUMO). This energy gap (5.0371eV) between the two molecular orbitals agreed with the energy band gap (5.6529eV) calculated from FMO [26]. Fig .5 Shows theoretical UV–vis spectrum of the title compound.

λ_{max} (nm)	Band gap (eV)	Energy (cm-1)	f	Assignments
246.1696	5.037177	40622.39	0.0341	HOMO->LUMO (90%)
240.9549	5.146192	41501.54	0.0006	HOMO->L+1 (93%)
233.6135	5.30007913	42805.75	0.0036	H-2->LUMO (20%), H-2->L+1 (17%), H-1->LUMO (29%), H-1->L+1 (26%)

Table 5: Theoretically calculated electronic properties using the TD-DFT method.

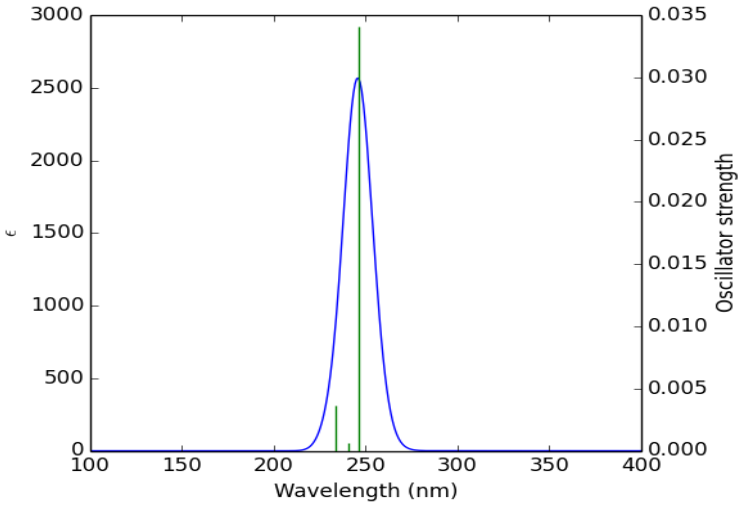

Figure 5: theoretical UV–vis spectrum of the title compound.

Molecular Electrostatic Potential

The distribution of charges over a 3-dimensional space creates an electrostatic potential around it. MEP also known as molecular electrostatic potential explains us about how the molecule would react to charges surrounding it. The mapping of MEP was done

with DFT methods along with basis set B3LYP/6-311++G (d, p) [27]. There are two major sites in a molecule namely electrophilic sites wherein the atoms in this region have tendency to attract electrons and nucleophilic sites wherein the atoms in this region are ready to share electrons. MEP diagram is shown in Fig.6. The colour region varies from red to blue where red signifies electrophilic site and blue signifies nucleophilic site. Potential in the current study ranges from - $4.002e^{-2}$ eV to $4.002e^{-2}$ eV. From the figure, the red region denotes electrophilic region which is due to the presence of N21 atom [28,29]. The blue region at the borders constitutes nucleophilic sites. H atoms occupying this region are nucleophilic in nature. The green site in map indicates neutral sites.

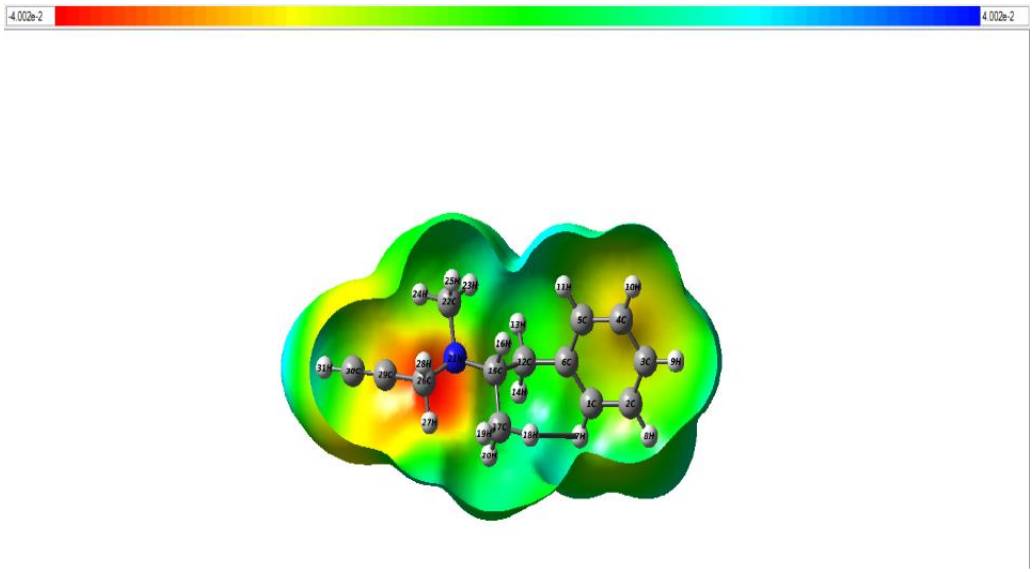

Figure 6: The MEP map of the title compund.

Electron Localization Function & Local Orbital Locator

Topological analyses of ELF and LOL were carried out using MULTIWFN software [30]. The 2D mapped ELF and LOL is shown in fig. 7 and fig. 8. The colour codes vary from 0.001 to 1.000. High ELF values are represented by red region whilst low ELF values are represented by blue region [31]. The main objective to perform ELF studies is to understand quantitative behaviour of electrons in a system. The difference in kinetic energy density contributes towards Pauli repulsion on two like spin electrons which attributes towards the behaviour of the electron. The red region indicates high Pauli repulsion, and blue region indicates low Pauli repulsion [32]. Several colours are represented on this surface. For the title compound, blue colour circle in 2d structure, indicates the presence of a depletion region between valence shell and inner shell.

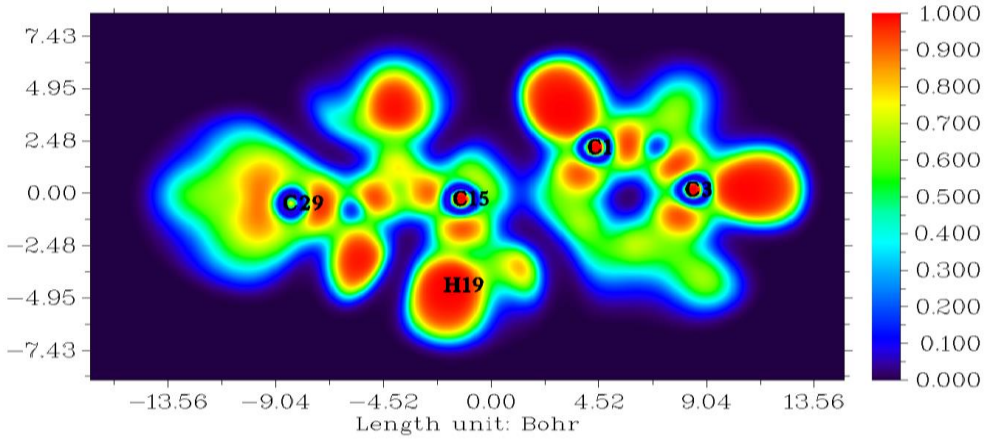

Figure 7: The 2-D mapped ELF for the title compound.

The red orange region depicts strong electronic localisation [33,34]. Localized orbital locator is like that of ELF. The hydrogen and carbon regions have minimum values of LOL. The LOL has colour codes ranging from 0.000 to 0.800 [35]. The white region encircled with red region of H19 atom indicates that there is an excess of electron cloud which exceeds the covalent region.

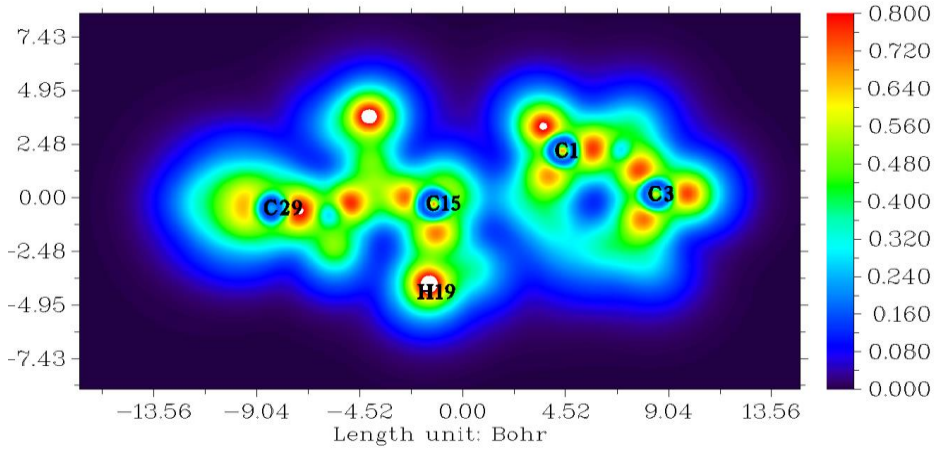

Figure 8: The 2-D mapped LOL for the title compound.

Drug Likeness

The canonical smile of selegiline was taken from PubChem [36]. Using this, Drug likeness parameters tabulated in table 8 was obtained by SwissADME software [37]. The acceptable values of HBA and HBD should be less than 5 and 10 respectively, which is 1 and 0 for the title compound. The MlogP parameter gives an idea about lipophilic character of the molecule, which is 3.25 for the title compound. This is in the acceptable range as it is less than 4.15. The number of rotatable bonds should be less than 10 and is 4 in this case. Based on the analysis, the title compound satisfies Lipinski's rule of five most likely favourable to be subjected to any desired studies since it proves that it is an active drug. [38]

Descriptors	Value
Hydrogen bond donors (HBD)	0
Hydrogen bond acceptors (HBA)	1
ALogP	3.25
Polar surface area (PSA) $Å^2$	3.24
Molar refractivity	61.31
Number of atoms	31
Number of rotatable bonds	4

Table 8: Descriptors and corresponding values for drug likeness of the title compound.

Molecular Docking

Molecular docking of the title compound was carried out using AutoDock software. Protein used for docking was taken from protein data bank (PDB). Optimised docked structure of target protein with the title compound is shown in fig. 9. Protein had a resolution of 2.30 Å [39]. Protein structure was obtained from RCSB PDB format. Auto dock tool (ADT), a graphical user interface was used to obtain binding energy of the title compound to a receptor. The title compound was selected to be docked into the active site of protein 4f1t (Parkinson's disease). Docking parameters such as Bond distance (Å), Inhibition constant (μm), Intermolecular energy (kcal/mol), Binding Energy (kcal\mol) and Reference RMSD (Å) are tabulated in table 7. Minimum binding energy of – 3.61 kcal/mol and intermolecular energy of −4.8 kcal/mol have been observed in the interaction which interprets that protein and the title compound has strong bond between them. Inhibition constant and bond distance found to be 2.27 μm and 2.631 Å respectively [40].

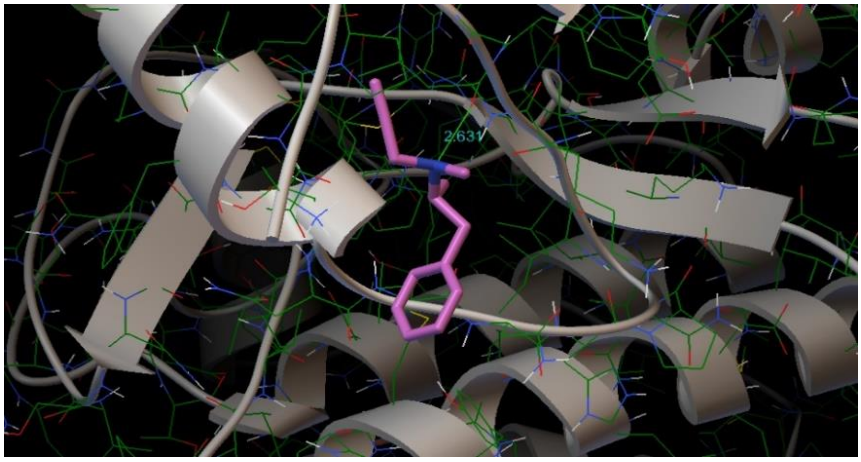

Figure 9: Optimised docked structure of the target protein with the title compound.

Protein	Bonded residues	Bond distance Å	Inhibition constant μm	Intermolecular energy kcal/mol	Binding Energy kcal\mol	Reference RMSD Å
4f1t	LEU1093	2.631	2.27	-4.8	-3.61	19.67

Table 7: Docking parameters of the protein 4f1t with the title compound.

Conclusion

In the present work, a detailed Spectroscopic (FT-IR, FT-RAMAN), UV, FMO, Reactive site analysis (MEP, ELF, LOL) along with molecular docking studies on the title compound, Selegiline has been reported. Optimized molecular geometry was obtained using DFT method along with basis set B3LYP/6-311++G (d, p). The complete vibrational assignments and calculations of potential energy distribution (PED) were carried out using Veda software. Reactive sites of the title compound were determined using LOL and ELF. From MEP diagram, the electrophilic and nucleophilic sites were identified. Electronic properties of the compound were studied theoretically using TD-DFT method. Energy gap calculated from UV spectrum was in good agreement with HOMO-LUMO energy gap. Finally, molecular docking analysis was carried out for protein 4flt associated with Parkinson's disease and showed binding affinity value of -3.61 kcal/mol.

References

1. Youdim MDH, Riederer PF (2004) A review of the mechanisms and role of monoamine oxidase inhibitors in Parkinson's disease. Neurology 63: S32-S35.
2. Youdim MDH, Edmondson D, Tipton KF (2006) The therapeutic potential of monoamine oxidase inhibitors. Nature reviews neuroscience 7: 295-309.
3. Gerlach M, Youdim MBH, Riederer P (1996) Pharmacology of selegiline. Neurology 47: 137S-145S.
4. Ward CD (1994) Does selegiline delay progression of Parkinson's disease? A critical re-evaluation of the DATATOP study. Journal of Neurology, Neurosurgery & Psychiatry 57: 217-220.
5. Salonen JS, Nyman L, Boobis AR, Edwards RJ, Watts P, et al. (2003) Comparative studies on the cytochrome p450-associated metabolism and interaction potential of selegiline between human liver-derived in vitro systems." Drug metabolism and disposition 31: 1093-1102.
6. Gnanasambandan T, Gunasekaran S, Seshadri S (2013) Quantum Chemical and Spectroscopic (FT-IR, FT-Raman) Study, First Order Hyperpolarizability, NBO, Analysis HOMO and LUMO Analysis of Selegiline by abinitio HF and DFT Method. Oriental Journal of Chemistry 29: 185.
7. Becke AD (1994) Density-fumctional exchange energy approximation with correct asymptotic behavior. Phys. Rev. B: 54.
8. Perdew JP, Burke K, Wang Y (1996) Generalized gradient approximation for the exchange-correlation hole of a many electron system. Phys. Rev. B: 54.
9. Chemcraft – graphical software for visualization of quantum chemistry computations.
10. Jamroz MH (2004) Vibrational Energy Distribution Analysis: VEDA 4 Program, Warasaw, Poland.
11. Roy D, Keith T, Millam J, GaussView, Semichem Inc., Shawnee Mission, KS, 2009. Version 5.
12. Politzer P, Truhalr DG (Eds.), Chemical Application of Atomic and Molecular Electrostatic Potential, Plenum, Newyork, 1981.
13. Mulliken RS (1934) A new electronaffinity scale; Together with Data on valence states and on valence ionization potentials and electron affinities. J. Chem. Phys. 2: 782-793.
14. Tian Lu, Chen F (2012) Multiwfn: a multifunctional wavefunction analyzer. J. Comp. Chem 33: 580-592.
15. Antoine D, Michielin O, Zoete V (2017) SwissADME: a free web tool to evaluate pharmacokinetics, drug-likeness and medicinal chemistry friendliness of small molecules." Scientific reports 1: 1-13.
16. Tanchuk V, Tanin V, Vovk A (2013) Multithreaded version of AutoDock 4.2 suitable for massive virtual screening of potential biologically active compounds (enzyme inhibitors)." Third International

Conference" High Performance Computing" HPC-UA.
17. Fathima RB, Johanan CP, Muthu S (2017) Spectroscopic investigation (FT-IR, FT-Raman, UV, NMR), Computational analysis (DFT method) and Molecular docking studies on 2-[(acetyloxy) methyl]-4-(2-amino-9h-purin-9-yl) butyl acetate. Int. J. Mater. Sci 12: 196-210.
18. WebSpectra.
19. IR Spectroscopy Tutorial: Amines.
20. Barnes AJ, Majid MA, Stuckey MA, Gregory P, Stead CV (1985) The resonance Raman spectra of Orange II and Para Red: molecular structure and vibrational assignment. Spectrochimica Acta Part A: Molecular Spectroscopy 41: 629-635.
21. Joe IH, Kostova I, Ravikumar C, Amalanathan M, Cîntă Pînzaru S (2009) Theoretical and vibrational spectral investigation of sodium salt of acenocoumarol. Journal of Raman Spectroscopy: An International Journal for Original Work in all Aspects of Raman Spectroscopy, Including Higher Order Processes, and also Brillouin and Rayleigh Scattering 40: 1033-1038.
22. Ramazani A, Sheikhi M, Yahyaei H (2017) Molecular Structure, NMR, FMO, MEP and NBO Analysis of Ethyl-(Z)-3-phenyl-2-(5-phenyl-2H-1, 2, 3, 4-tetraazol-2-yl)-2-propenoate Based on HF and DFT Calculations. Chemical Methodologies 1: 28-48.
23. Rizwana F, Prasana JC, Muthu S, Abraham CS (2019) Molecular docking studies, charge transfer excitation and wave function analyses (ESP, ELF, LOL) on valacyclovir: a potential antiviral drug. Computational biology and chemistry 78: 9-17.
24. Manjusha P, Prasana JC, Muthu S, Rizwana FB (2019) A computational and spectroscopic interpretation (FT-IR, FT-Raman, UV–vis and NMR) with molecular docking studies on 3-carboxy-2-hydroxy-N, N, N-trimethyl-1-propanaminium hydroxide: A pharmaceutical drug. Chemical Data Collections 20: 100191.
25. Geoffrey BAS, Prasana JC, Muthu S, Abraham CS, et al. (2019) Spectroscopic and quantum/classical mechanics based computational studies to compare the ability of andrographolide and its derivative to inhibit nitric oxide synthase. Spectrochimica Acta Part A: Molecular and Biomolecular Spectroscopy 218: 374-387.
26. Fathima Rizwana B, Johanan CP, Muthu S (2017) Spectroscopic investigation (FT-IR, FT-Raman, UV, NMR), Computational analysis (DFT method) and Molecular docking studies on 2-[(acetyloxy) methyl]-4-(2-amino-9h-purin-9-yl) butyl acetate. Int. J. Mater. Sci 12: 196-210.
27. Marinho ES, Marinho MM (2016) A DFT study of synthetic drug topiroxostat: MEP, HOMO, LUMO." International Journal of Scientific & Engineering Research 7: 8.
28. Fathima Rizwana B, Muthu S, Johanan CP, Abraham CS, Raja M (2018) Spectroscopic (FT-IR, FT-Raman) investigation, topology (ESP, ELF, LOL) analyses, charge transfer excitation and molecular docking (dengue, HCV) studies on ribavirin. Chemical Data Collections 17: 236-250.
29. Prabakaran M, Prasana JC (2021) Molecular docking studies, natural bond orbital, charge transfer excitation, NLO, ELF, LOL, and drug likeness analysis on Cefixime: a potential anti-bacterial effective. Sci Academique 2: 1-18.
30. George J, Prasana JC, Muthu S, Kuruvilla TK, Saji RS, et al. (2020) Evaluation of vibrational, electronic, reactivity and bioactivity of propafenone—A spectroscopic, DFT and molecular docking approach. Chemical Data Collections 26: 100360.
31. Noureddine O, Issaoui N, Medimagh M, Al-Dossary O, et al. (2021) Quantum chemical studies on molecular structure, AIM, ELF, RDG and antiviral activities of hybrid hydroxychloroquine in the treatment of COVID-19: Molecular docking and DFT calculations. Journal of King Saud University-Science 33: 101334.

32. Saji RS, Prasana JC, Muthu S, George J, Kuruvilla TK, et al. (2020) Spectroscopic and quantum computational study on naproxen sodium. Spectrochimica Acta Part A: Molecular and Biomolecular Spectroscopy 226: 117614.
33. Radder SB, Melavanki R, Hiremath SM, Kusanur R, et al. (2021) Synthesis, spectroscopic (FT-IR, FT-Raman, NMR & UV-Vis), reactive (ELF, LOL, Fukui), drug likeness and molecular docking insights on novel 4-[3-(3-methoxy-phenyl)-3-oxo-propenyl]-benzonitrile by experimental and computational methods. Heliyon 7: e08429.
34. Pilepić V, Uršić S (2001) Nucleophilic reactivity of the nitroso group. Fukui function DFT calculations for nitrosobenzene and 2-methyl-2-nitrosopropane. Journal of Molecular Structure: THEOCHEM 538.1-3: 41-49.
35. Manju P, Muthu S, Gowda NMN (2017) Quantum mechanical and spectroscopic (FT-IR, FT-Raman, 1H, 13C NMR, UV-Vis) studies, NBO, NLO, HOMO, LUMO and Fukui function analysis of 5-Methoxy-1H-benzo [d] imidazole-2 (3H)-thione by DFT studies. Journal of Molecular Structure 1130: 511-521.
36. Compound Summary. Selegiline
37. http://www.swissadme.ch/index.php
38. Saji RS, Prasana JC, Muthu S, George J, Kuruvilla TK, et al. (2020) Spectroscopic and quantum computational study on naproxen sodium. Spectrochimica Acta Part A: Molecular and Biomolecular Spectroscopy 226: 117614.
39. https://www.rcsb.org/structure/4F1T
40. Manjusha P, Prasana JC, Muthu S, Rizwana BF (2019) A computational and spectroscopic interpretation (FT-IR, FT-Raman, UV–vis and NMR) with molecular docking studies on 3-carboxy-2-hydroxy-N, N, N-trimethyl-1-propanaminium hydroxide: A pharmaceutical drug. Chemical Data Collections 20: 100191.